J. Sens. Actuator Netw. **2012**, *1*, 3-35; doi:10.3390/jsan1010003

OPEN ACCESS

Journal of Sensor and Actuator Networks

ISSN 2224-2708

www.mdpi.com/journal/jsan/

Article

A Discrete Wavelet Transform (DWT)-Based Energy-Efficient Selective Retransmission Mechanism for Wireless Image Sensor Networks

Daniel G. Costa [1,2,]* and Luiz Affonso Guedes [1]

[1] DCA-CT-UFRN, Campus Universitário, Lagoa Nova, Federal University of Rio Grande do Norte, 59072-970 Natal RN, Brazil; E-Mail: affonso@dca.ufrn.br

[2] DTEC-UEFS, Av Transnordestina, S/N, Novo Horizonte, State University of Feira de Santana, 44036-900 Feira de Santana BA, Brazil

* Author to whom correspondence should be addressed; E-Mail: danielgcosta@uefs.br; Tel.: +55-84-8827-1120.

Received: 8 December 2011; in revised form: 16 January 2012 / Accepted: 29 January 2012 / Published: 1 February 2012

Abstract: Source nodes in wireless image sensor networks transmit much more information than traditional scalar sensor networks, thereby demanding more energy of intermediate relaying nodes and putting energy efficiency as a key design issue. Intermediate nodes are usually interconnected by error-prone links where bit-errors are common, potentially degrading the application monitoring quality. When reliability is assured by retransmission mechanisms, higher packet error rates do not affect the application quality but result in additional energy consumption due to packet retransmission, even though many monitoring applications can tolerate some loss in the quality of the received image. DWT coding can decompose an image in data subbands, each one with different relevancies for the reconstruction of the original image at the receiver side. We propose an energy-efficient selective hop-by-hop retransmission mechanism where the reliability level of each packet is a function of the relevance of the payload data, according to the resulting subbands and the number of times a 2D DWT is applied over the images captured by the sensors' cameras. In so doing, some lost packets are not retransmitted, saving energy of intermediate nodes with low impact to the quality of the reconstructed images. In order to estimate the benefits of this tradeoff between energy consumption and image quality, we designed a comprehensive energy consumption model and applied it in extensive mathematic simulations, providing substantial information about the mean performance of the proposed approach when compared with a fully-reliable transmission mechanism.

Keywords: wireless image sensor networks; DWT; hop-by-hop retransmission; energy-efficiency; wireless sensor networks

1. Introduction

In recent years, Wireless Sensor Networks (WSNs) have raised a lot of attention of the industry and academic communities [1], addressing applications as surveillance, tracking, disaster monitoring, home automation, industrial control, battlefield surveillance, among others. Typically, WSNs are composed of many self-organizing disposable electronic devices equipped with a short-range wireless transceiver, limited energy supply (usually batteries), a sensing unity and processing and memory resources [2,3]. When deployed over an area of interest, sensors can collect scalar information as humidity, pressure, temperature, luminosity and seismic variations, according to the application requirements and the nature of the sensing unit endowed in each source node [4,5].

The use of low-cost, low-power and low-resolution cameras to collect visual information can strongly enhance the monitoring capability of such networks, allowing for the development of Video-based Wireless Sensor Networks (VWSNs) [6,7]. However, such visual monitoring capability imposes some challenges due to the resource-constrained nature of wireless sensors, since transmissions of visual data usually require higher communication bandwidth than transmissions of scalar data. In addition, source nodes need to process multimedia encoding algorithms and reliable communication is required for most VWSNs applications due to the lack of redundancy when video-based sensors are employed [8,9]. As an example of how such a communication scenario can be challenging: while few bytes can represent monitored scalar information, such as humidity, pressure and temperature, a small uncompressed 128 × 128 pixels 8-bit grayscale image is represented by 16,384 bytes (excluding the image header), demanding more bandwidth and potentially consuming more energy of intermediate nodes than scalar data. In such contexts, the resource-constrained hardware of modern wireless sensor motes [4] and the limited transmission bandwidth imposed by LR-WPAN communication technologies as IEEE 802.15.4 will render visual monitoring by still images a more suitable option for most video-based wireless sensor networks, since video transmission may rapidly deplete the energy resources of the nodes or be even unfeasible for transmissions from multiple sources through braided paths. The sensor networks where source nodes transmit still images and optionally some complementary scalar data can be referred to as Wireless Image Sensor Networks (WISNs).

When transmitting image packets over error-prone wireless links, packets can be corrupted, and can require retransmission. In wireless image sensor networks, the lack of redundancy and the unique view of source sensors over the monitored field [9] turn the recovery of lost packets into a required service, since the desired view of a target may be only achieved by a unique source node. Additionally, some parts of the visual information transmitted from source nodes may be extremely relevant for the decoding process at the sink node. Data link technologies such as IEEE 802.15.4 retransmit corrupted packets, where correct reception is usually acknowledged in each link between intermediate nodes. As packet transmission consumes energy of the receiving and transmitting nodes, we can establish a direct relation between energy consumption and packet retransmission. In other words, when the packet error rate increases, more energy consumption is expected due to packet retransmission, but with very low or absent impact in the quality of the visual data received by the sink. While such behavior may be acceptable for traditional scalar sensor networks, some visual applications can afford loss in the image quality since the overall energy of the network is preserved.

Camera-enabled source nodes can encode still images using Discrete Wavelet Transform (DWT). In short, DWT decomposes the original image in subbands with different relevancies for the reconstruction of the original image. As a result, packets will have different priorities for the applications depending on the carried information, and such priorities may be exploited by cross-layer optimization solutions [10]. In such contexts, we propose a DWT-based selective retransmission mechanism where reliable transmission is only assured for the most relevant data to the application, while low relevant packets are not retransmitted if they are discarded due to corruption during transmission. When the packet error rate is low, most data will reach the sink, resulting in high-quality images. On the other hand, increasing in the packet error rate will decrease the image quality since lost low-relevant packets will not be retransmitted. We believe that, for many WISN applications, reduction in the image quality is acceptable since energy is preserved.

The proposed approach assumes that the images gathered by the source nodes are encoded using a DWT-based technique, where the information carried by each packet through a multi-hop network has its own relevance for the application. Thus, the source nodes establish a priority level to every packet transmitted to the sink. Based on such priorities, the network can provide three different transmission services: reliable, semi-reliable and unreliable. The adopted transmission service is reflected on the way intermediate nodes process corrupted packets, which can be retransmitted or silently discarded. It is assumed that source nodes transmit only still images or scalar data, but the operation of the transmission services could be easily adapted if video streaming is required, depending on the application requirements and the adopted video coding technique.

In order to assess the expected benefits, we designed a comprehensive energy consumption model to be applied in extensive mathematic simulations, showing the average results for different network configurations. Additionally, the expected image quality when some packets are lost and not retransmitted is analyzed.

The rest of this paper is organized as follows. Section 2 brings some related works that contributed to our investigation. The problem formulation is presented in Section 3. Section 4 describes the proposed selective retransmission solution, followed by mathematical verifications in Section 5. Finally, the conclusions and references are presented.

2. Related Works

While most real-time multimedia communications on Internet backbones are delay-intolerant and can generally afford some packet loss, reliability is more critical to image transmissions over WSNs than delay. Usually, errors during packet transmission over hop-by-hop wireless links may happen when network face congestion (resulting in packet discarding in congested nodes), when intermediate nodes fail or run out of energy or even due to signal attenuation and interference. To cope with such errors, many works have proposed MAC and transport protocols to recover lost packets/data in wireless sensor networks, where retransmission is the most usual approach.

Retransmission can be performed in an end-to-end or hop-by-hop fashion. End-to-end retransmission is easier to implement but can rapidly deplete the energy resources of the used paths as the number of intermediate nodes increases. A hop-by-hop retransmission mechanism consumes less energy of the network, but demands that intermediate nodes cache the transmitted packets until the transmission is successful. Although this additional complexity may count against hop-by-hop retransmissions, it is argued to be the best option for source nodes that transmit a large amount of data, as in video-based wireless sensor networks [4,11].

An end-to-end retransmission mechanism for WSN applications is proposed in [12]. The sink verifies the sequence number of received packets searching for some packet loss. If a gap in the sequence number is found, an explicit request is sent to the source node requesting retransmission of the lost packet. In a different way, in [13] a transport protocol is proposed that performs in-network caching of transmitted packets for hop-by-hop retransmission. In that work, packet loss is identified by proper timers enabled in intermediate nodes and notifications are performed by explicit NACK messages sent to the next hop on the reverse reinforced path toward the source. Moreover, the work in [14] employs multiple redundant paths as well as hop-by-hop retransmission for increased reliability, where congestion is also mitigated dynamically choosing appropriate transmission paths. Although very advantageous for VWSNs, all packets have the same reliability level in those proposed hop-by-hop retransmission mechanisms.

Alternative solutions to provide reliability guarantees have also been proposed in recent years. In [15], authors propose image transmission over sensor networks where intermediate nodes perform error recovery based on redundancy and correction codecs. As retransmissions may result in additional end-to-end delay, the authors propose correction mechanisms based on the transmission of redundant packets through multiple paths and the use of Forward Error Correction (FEC) codes, which are computed by each intermediate node instead of only in the source node and in the sink. However, the reduced end-to-end delay when compared with retransmission-based approaches also result in additional energy consumption, since more paths (and intermediate nodes) are necessary to transmit redundant packets, besides the energy consumption and required processing for computing the FEC code in intermediate nodes. In fact, we argue that energy is a more critical issue than delay for many WVSN applications.

To the best of our knowledge, a mechanism for selective retransmission based on DWT coded images has not been proposed by the academic community [10]. However, some works propose other interesting cross-layer optimization solutions for DWT-based image transmission in wireless sensor networks, directly influencing our investigation. In [16] full reliable transmission is only required for high-priority data, since the remaining DWT subbands are transmitted in a semi reliable mode, where intermediate nodes silently discard low relevant packets if their residual energy is below a threshold. The expected outcome is the prolonging of the network lifetime, keeping an acceptable quality level for the received images. The work in [17] exploits DWT to reduce the total amount of information to be transmitted to the sink when facing congestion, with a low impact on the overall quality of the application. In case of congestion, priorities resulted from the different relevancies of DWT subbands are considered by intermediate nodes. The idea is to discard packets containing less relevant data when the congested node may choose what packets must to be discarded.

All those works exploit DWT in different ways, achieving different optimization results. In a similar way, DWT image coding is exploited here for cross-layer optimization in video-based wireless sensor networks, but we propose an innovative retransmission service where the relevancies of DWT subbands are considered by intermediate nodes for retransmission purposes, achieving energy saving by the cost of some loss of image quality.

3. Problem Formulation

In this section we make some basic definitions and assumptions that are considered for the design of the proposed DWT-based selective retransmission mechanism.

3.1. Packet Retransmission

When camera-enabled source nodes are transmitting still images over error-prone wireless links, packets can be corrupted requiring retransmission. As stated before, the lack of redundancy and the unique view of source sensors over the monitored field [9] turn recovery of lost packets into a required service. Additionally, some parts of the visual information transmitted from source nodes may be extremely relevant for the decoding process at the sink, such as $LL_{(n)}$ DWT subbands. Data link technologies such as IEEE 802.15.4 [3] and T-MAC [18] retransmit corrupted packets, where correct reception is usually acknowledged in each link between intermediate nodes. In general, higher packet error rates and packet retransmissions result in higher energy consumption.

There are different data recovery mechanisms for wireless sensor networks [10]. Among the possibilities, we consider packet retransmission as a suitable option for wireless image sensor network, where hop-by-hop retransmission will be implemented instead of end-to-end approaches for increased energy saving [4,14]. For simplicity and considering the use of contention-free MAC protocols, we assume that every transmitted packet in a link will be acknowledged by a 1-hop ACK message. This Automatic Repeat Request (ARQ) approach is an easy way to provide a reliable communication service in WSNs, although some technologies as T-MAC may employ ACK messages that can acknowledge more than one packet at once. Nevertheless, our theoretical formulation is reasonable due to the reduced complexity and because this approach is suitable for error-prone wireless links. Figure 1 shows an example of ARQ in a single-path transmission.

Figure 1. ACK messages in hop-by-hop packet retransmission.

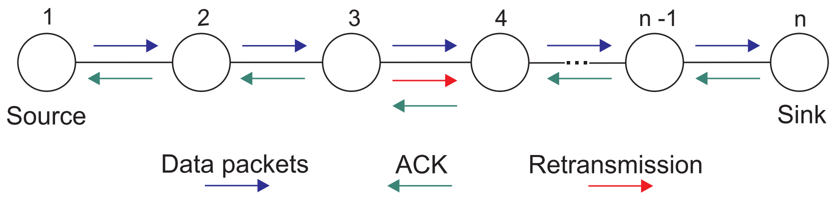

In Figure 1, packet transmission flows from node 1 to node *n*, and a packet corruption happens during transmission from node 3 to node 4. When no ACK message is received before a timeout, the packet is assumed to be corrupted and a retransmission takes place. Recovery of lost packets through retransmission is suitable for most wireless sensor network applications, preserving the transmitted packets by the cost of additional energy consumption and end-to-end communication delay.

Intermediate nodes will transmit packets using a FIFO transmission queue. Considering that the communication between intermediate nodes will be half-duplex due to the fact that they will be typically endowed with only one wireless communication antenna, the communication is expected to follow a "stop-and-wait" paradigm, where the packet at the top of the queue is only removed if it is successfully acknowledged by the next hop toward the sink.

3.2. Fundamental Concepts for Energy Consumption

We consider a WSN composed of P hop-by-hop wireless paths. Each path p, $p = 1, \ldots, P$, comprises H_p intermediate nodes, where data packets flow from the source node ($h = 0$) to the sink of the network ($h = H_p + 1$). A number of D_p data packets are transmitted in each path p. The size of the transmitted packets may vary according to the link layer technology and the application requirements, but small data packets are expected (reducing the error probability [19]) with the same size. Considering that most wireless sensor motes communicates through IEEE 802.15.4 wireless link-layer technology, the maximum MAC frame size is assumed to be 127 bytes including all packet overhead. If we exclude the MAC header and the overhead for network, transport and/or application layer protocols, as well as the image fragmentation header required for image decoding at the receiver size, the effective data size in each packet may be lower than 90 bytes in this link-layer technology [20]. Considering that even a very small 64 × 64 uncompressed grayscale image sizes 4,096 bytes (excluding the image header of the entire image), it is natural to expect transmission of packets with maximum size to achieve a minimal packet overhead. Thus, in our model, every data packet has the same size in bits, s, corresponding to the entire packet (data payload + headers), since all transmitted bits should be considered when computing the expected energy consumption. This initial idea is further extended to account the expected reduced size of the last packet after fragmentation, as described later in this section.

For simplicity, the communication scenario is assumed to be contention-free, considering packet transmission using protocols as TDMA or the CFP (Contention-Free Period) in IEEE 802.15.4. Such assumption is intended to reduce the complexity of our mathematic models, but still keeping it highly realistic, following a trend often found in the literature [15,16,21]. Although not explicitly defined, the routing protocol may be cluster-based, allowing the creation of hop-by-hop paths from the source to the sink node. Moreover, node failure or harming were not considered. A large set of image-based WSN monitoring applications or even traditional scalar monitoring applications where the collected information is complemented by visual data attend such requirements.

Considering that it is highly probable that all intermediate nodes in a path p are homogeneous (excepting the source and the sink), we can expect the same hardware characteristics and energy consumption pattern. Based on [15], e_t is defined as the energy consumed for the transmission of one bit by each relaying node, and e_e as the energy consumption for processing of a single bit. The energy consumption for packet transmissions (Et_{ph}) and receptions (Er_{ph}) in an intermediate node h of the path p is a function of the energy consumption characteristics of the employed hardware and the total amount of bits to be transmitted/received, as expressed in Equation (1). The variable d_{ph} is the maximum transmission range (in meters) of the node h, and it is a direct function of the sensor's hardware. T_{ph} is the total amount of bits to be transmitted from hop h to the hop $(h + 1)$ in path p, and $T_{ph} = D_p \times s$ when there are no packet retransmission.

$$\begin{aligned} Et_{ph} &= T_{ph}.\left(e_e + e_t.d_{ph}^2\right) \\ Er_{ph} &= T_{p(h-1)}.e_e \end{aligned} \tag{1}$$

As most energy consumption is expected in transmission and reception procedures instead of processing and storage [21–23], we can roughly state the total energy consumption in path p as expressed in Equation (2). The total consumed energy is the sum of the energy consumption in transmission and reception in all intermediate nodes ($h = 1, \ldots, H_p$), plus the energy for transmissions from the source node ($h = 0$) and reception of data packets at the sink ($h = H_p + 1$). As the sink is expected to be resource-full, the corresponding energy was not considered.

$$E_p = \sum_{h=1}^{H_p}\left(Et_{ph} + Er_{ph}\right) + T_{p0}.\left(e_e + e_t.d_{p0}^2\right) \tag{2}$$

3.2.1. Error Model

Packets in WSNs may be discarded for many reasons, as congestion, node failure and optimization mechanisms [10]. Moreover, multiple accesses to the communication medium may also result in packet collision, requiring a MAC protocol to handle the shared access to the channel and to retransmit collided packets. In such cases, many works have proposed solutions to recover lost data or to minimize the impact of packet loss in the final quality of the received data at the sink [4,15,24].

Wireless sensor networks are composed of resource-constrained nodes interconnected by ad-hoc wireless links that are expected to be deployed in regions with diverse characteristics, where signal interference may be a constant. Due to the nature of packet transmission over wireless links, communications also face channel fading. Such characteristics result in bit-errors that may happen in any part of the communication and in any hop from the source to the sink. Bit-errors resulting from transmission over wireless links is an inner characteristic of radio communications that directly results in packet losses, while the other causes of data loss depends on the employed sensor hardware, unexpected physical harming and/or the procedures of the physical/MAC protocols. For example, IEEE 802.15.4 allows the transmission of packets controlled by a slotted CSMA/CA protocol to handle packet collision but most or even all multimedia content can be transmitted during a Contention Free Period (CFP), where source nodes have dedicated access to the communication channel and frames do not collide [25]. As we are designing a generic solution for selective hop-by-hop retransmission, we are exclusively concerned with bit-errors and packet losses resulted from the characteristics of wireless communications.

Errors in wireless links will happen as bursts [19,25]. Although it is simpler to define the same error probability for every transmitted bit in a theoretical model, it is not practical for real-world applications since the error rate depends on the size of the packets [19]. The Gilbert/Elliot error model defines a Markov chain with two states: "good" and "bad". For simplicity, all the bits are unchanged in the good state, while in the bad state at least one of the bits is corrupted [26]. Figure 2 presents the Gilbert/Elliot Markov chain, where g is the probability to stay in good state and b is the probability to stay in the bad state.

Figure 2. Gilbert/Elliot Markov chain.

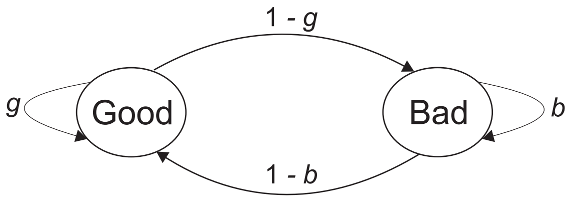

This error model refers to the transmission of bits in a wireless link connecting two nodes, and the values for g and b depend on physical characteristics of the considered link. Although this model refers to bit-errors, an error in a single bit will corrupt a whole packet, requiring retransmission. As we want to measure the energy consumption for packet transmissions and possible retransmissions, we are concerned with the average Packet Error Rate (PER) for transmitted packets from hop h to hop $(h + 1)$ in path p, Pn_{ph}, considering the transmission of n bits. For that, we need to compute the steady-state probability to good (G_{ph}) and bad (B_{ph}) states [26] in the wireless link from hop h to hop $(h + 1)$ in path p, as presented in Equation (3).

$$G_{ph} = \frac{1 - b_{ph}}{2 - (g_{ph} + b_{ph})}$$
$$B_{ph} = \frac{1 - g_{ph}}{2 - (g_{ph} + b_{ph})} \tag{3}$$

Based on these probabilities, we can compute the average PER for a packet with n bits (Pn_{ph}), as expressed in Equation (4). Such formulation is obtained considering the two cases where no bit error occurs during a transmission of a packet: the channel is in a good state and remains there for the entire transmission or the channel is initially in a bad state but the channel changes to a good state before transmission and remains in good state for the transmission of all bits [26].

$$Pn_{ph} = 1 - \left(G_{ph} . g_{ph}^{n} + B_{ph}(1 - b_{ph})g_{ph}^{n-1}\right) \tag{4}$$

For simplicity, we define Pt_{ph} as the PER for data packets ($n = s$) in the link from hop h to hop $(h + 1)$ in path p. Additionally, it is assumed that $Pn_{ph} = 0$ if $n = 0$.

3.2.2. Energy Consumption due to Packet Retransmission

We can extend the basic equations for energy consumption adding the energy costs for transmissions and receptions of 1-hop ACK messages when the communications links are free of errors. For simplicity and considering the use of contention-free MAC protocols, we assume that every transmitted packet in a link will be acknowledged by an ACK message. Such simplification facilitates the desired mathematical verifications, even though some MAC protocols employ ACK messages that can acknowledge more than one packet at once. As comparisons are required among different approaches using the same model, such simplification will not prejudice the desired analyses. Nevertheless, the presented theoretical formulation is reasonable due to the reduced complexity and because this approach is suitable for error-prone wireless links.

If we define the size of ACK messages in bits as a and A_{ph} as the total amount of bits to be transmitted for acknowledgement from hop $(h + 1)$ to hop h in path p, and $A_{ph} = D_p \times a$, we achieve new equations for energy consumption, as presented in (5). We expect $s > a$ in most cases.

$$\begin{aligned} Et_{ph} &= T_{ph}.\left(e_e + e_t.d_{ph}^2\right) + A_{p(h-1)}.\left(e_e + e_t.d_{p(h-1)}^2\right) \\ Er_{ph} &= e_e.\left(T_{p(h-1)} + A_{ph}\right) \end{aligned} \tag{5}$$

The resulting energy consumption equation for path p is defined in Equation (6). That equation takes into account the energy consumption for transmission of data packets and the corresponding ACK messages for the entire path (excluding transmission cost of the sink). One should notice that in Equation (6), bit-errors in the wireless communication links were not considered.

$$E_p = \sum_{h=1}^{H_p} \left(Et_{ph} + Er_{ph}\right) + T_{p0}.\left(e_e + e_t.d_{p0}^2\right) + A_{p0}.e_e \tag{6}$$

As it was computed the average packet error rate for transmitted packets, we can also estimate the average number of packet retransmissions. We define Pa_{ph} as the packet error rate for ACK messages $(n = a)$, and usually $Pt_{ph} > Pa_{ph}$ since we expect $s > a$.

A packet must be retransmitted in some particular cases. The first case is when the packet is corrupted in transmission from hop h in path p with probability Pt_{ph}, usually detected by computation of the CRC code of the packet. The other possibility of retransmission is when the packet is successfully received by the hop $(h + 1)$ but the correspondent ACK message is lost with probability $((1 - Pt_{ph})Pa_{ph})$ [27]. Considering that the maximum number of retransmission attempts is r, the average number of data packet transmissions in the steady-state (initial packet transmission + retransmission attempts) of a single packet in any hop h is defined in Equation (7).

$$\begin{aligned} Rt_{ph} &= 1 + \left(\left(1 - Pt_{ph}\right).Pa_{ph} + Pt_{ph}\right) + \left(\left(1 - Pt_{ph}\right).Pa_{ph} + Pt_{ph}\right)^2 + \\ &\ldots \\ &+ \left(\left(1 - Pt_{ph}\right).Pa_{ph} + Pt_{ph}\right)^r \end{aligned} \tag{7}$$

If is considered an unlimited number of retransmissions, we obtain a geometric series that can be simplified to Equation (8).

$$Rt_{ph} = \frac{1}{1 - \left(\left(1 - Pt_{ph}\right).Pa_{ph} + Pt_{ph}\right)} \tag{8}$$

The probability of sending exactly one ACK message is $(1 - Pt_{ph})$, referring to the correct reception of a data packet. Moreover, errors in the packet transmission or in the ACK message, with subsequent retransmission, will also result in new transmissions of ACK messages. Following the same approach in Equation (7), the average number of ACK messages is computed to be transmitted by hop h in path p, as expressed in Equation (9).

$$Ra_{ph} = (1 - Pt_{ph}) + (1 - Pt_{ph})((1 - Pt_{ph}).Pa_{ph} + Pt_{ph}) + (1 - Pt_{ph}) \\ ((1 - Pt_{ph}).Pa_{ph} + Pt_{ph})^2 + \ldots + (1 - Pt_{ph})((1 - Pt_{ph}).Pa_{ph} + Pt_{ph})^r \quad (9)$$

If we also assume an unlimited number of retransmissions, we obtain a new geometric series that can be simplified to Equation (10).

$$Ra_{ph} = \frac{(1 - Pt_{ph})}{1 - ((1 - Pt_{ph}).Pa_{ph} + Pt_{ph})} \quad (10)$$

Although unlimited number of retransmissions may sound not practical, it allows for reasonable mathematical assumptions about the average number of retransmissions in the steady-state. Moreover, virtually unlimited retransmission attempts may be desired by some applications and there are some practical mechanisms to increase the maximum number of retransmissions in a sensor node [28].

Based on Equations (8) and (10), it is defined a new interpretation for the total number of transmitted bits for data (T_{ph}) and ACK messages (A_{ph}), as presented in Equation (11). These variables should be applied directly in Equation (6) for the computation of the total energy consumption in a path p in the occurrence of errors in wireless links.

$$T_{ph} = D_p.s.Rt_{ph} \\ A_{ph} = D_p.a.Ra_{ph} \quad (11)$$

3.2.3. Energy Consumption Model for Image Transmission

The analytical energy consumption model defined in Equations (6) and (11) represent reliable communications in sensor networks where every packet is acknowledged and retransmitted if necessary, considering a hop-by-hop approach implemented in MAC or transport layer. We can further extend this model to adapt to the transmission of images, where every image i, $i = 1, \ldots, i = I$, sizing B_i bits is transmitted from a source node to the sink. It was stated before that the (maximum) size in bits of data packet is s, but this size corresponds to the payload and all protocol headers. If the packet header regarding all employed protocols sizes k bits, $k < s$, the maximum effective payload size for every transmitted packet is $(s - k)$ bits. As $B_i >> s$ in most cases, the original image i will be fragmented, and a fragmentation header with f bits containing information for the decoding at the receiver side will be added to every packet. Moreover, an image i may have an image header, with i_o bits, providing information as the width and height of the image and the number of bits used to represent a pixel. Thus, the number of packets to be transmitted is $(B_i + i_o)/(s - k - f)$, with packets carrying data information to their maximum payload excepting the last one, which may be carrying less data than its capacity. We define D_{pi} as the number of packets to be transmitted sizing s bits. The last packet has Ld_{pi} as the payload size, $Ld_{pi} < (s - k - f)$. Defining the maximum packet payload as l, $l = (s - k - f)$, it is achieved the formulas for D_{pi} and Ld_{pi}, as expressed in Equation (12).

$$D_{pi} = \left\lfloor \frac{(B_i + i_o)}{l} \right\rfloor$$
$$Ld_{pi} = \left((B_i + i_o) - l.\left\lfloor \frac{(B_i + i_o)}{l} \right\rfloor \right) \tag{12}$$

Assuming Ptd_{ph} as the packet error rate in hop h when $n = (Ld_{pi} + s - l)$ in Equation (4), where $(s - l)$ is the total packet headers and overheads, it is obtained the average number of transmissions and retransmissions of the last packet in hop h, Rtd_{ph}, when employing Ptd_{ph} in Equation (8). This is necessary since the packet error rate is a function of the sizes of the packets. The probability of ACK transmissions is also affected by the possible smaller size of the last packet after fragmentation. Applying the value of Ptd_{ph} to Equation (10), it is obtained the average number of ACK messages to acknowledge the transmission of the last packet in hop h, Rad_{ph}. The new formulations for T_{pih} and A_{pih} for the transmission of an image i are presented in Equation (13). We define $Ptd_{ph} = 0$, $Rtd_{ph} = 1$ and $Rad_{ph} = 1$ if $Ld_{pi} = 0$.

$$T_{pih} = D_{pi}.s.Rt_{ph} + (Ld_{pi} + s - l).Rtd_{ph}$$
$$A_{pih} = a.(D_{pi}.Ra_{ph} + Rad_{ph}) \tag{13}$$

Using the definitions for T_{pih} and A_{pih} in Equation (13), the resulting equation in Equation (6) presents a comprehensive energy consumption model for transmission and reception of packets carrying parts of an image i in full reliable communications. The required energy for processing the original image was not accounted in this model, but a standard energy formulation for DWT processing will be considered in next section. Furthermore, the size B_i refers to a raw image i, but compression could be used to reduce the total amount of information to be transmitted, at the cost of processing and energy resources of source nodes. Image compression is not considered in this work but, in the case that compression is employed, lossless compression should be used since it is typically less complex and resource-demanding than lossy compression [16,29]. However, lossy algorithms could be exploited if resource-rich source nodes are deployed, achieving higher compression efficiency.

4. The Proposed Selective Retransmission Mechanism

The energy consumption model described in Section 3 refers to a fully-reliable hop-by-hop retransmission mechanism where all packets have the same treating by the nodes and every packet is acknowledged. When the packet error rises, the quality of the data received by the sink is preserved, but the energy consumption also increases, potentially impacting the expected network lifetime.

Energy is a crucial resource that must be saved as much as possible in order to extend the sensor network lifetime. Considering the context of wireless image sensor networks, we propose a selective hop-by-hop retransmission mechanism that can save energy by avoiding retransmission of some packets by the cost of the quality of the received image at the sink. It is expected that sensor nodes may be interconnected by error-prone wireless links where burst of errors may be constant, but temporary. In such context, we argue that some visual monitoring applications can tolerate some loss of quality in the received images, since the energy resources of intermediate nodes are preserved. Moreover, we expect that such applications are delay-tolerant and immune to jitter, since all parts of an image must to be buffered at the sink to allow the decoding process and typical transmission rate of visual information collected from the monitored field should be one snapshot per second or lower. However, the decision not to retransmit some corrupted packet results in less than average end-to-end delay, but we do not consider it to be crucial for some types of applications.

The proposed selective hop-by-hop retransmission mechanism is based on the relevance of the data resulted when we apply DWT over original images, where only the packets that carry the most significant information are retransmitted if corrupted. Doing so, we achieve a tradeoff between energy consumption and image quality, bringing a valuable contribution to wireless image sensor networks.

4.1. DWT-Based QoS

There are many coding techniques suitable for wireless image sensor networks, each one bringing advantages and drawbacks [10]. Among the possibilities, DWT has been considered by the academic community as a flexible option for image coding [30], allowing a series of cross-layer optimizations for energy preservation with low impact on the application general quality. In fact, when applied over images, DWT can produce data with different priorities, and such priorities can be reflected into QoS levels that can be exploited for network optimizations. If packets carrying less relevant information are lost, the image quality is lower-bounded, and an acceptable played-out image quality is assured at the receiver size if more relevant packets successfully reach the sink.

Wavelet transforms provide data decomposition in multiple levels of resolution, where DWT is achieved discretely sampling the wavelets. DWT decomposes a signal (a series of digital samples) by passing it through two filters: a lowpass filter L and a highpass filter H [30]. The lowpass subband represents a down-sampled low resolution version of the original signal, while the highpass subband contains residual information of the signal. For the perfect reconstruction of the original signal at the receiver side, all information from lowpass and highpass filters are necessary.

Digital images are two-dimensional signals, usually represented as a matrix of pixels. A 2D DWT processes such signal considering the rows and columns, generating four subbands: LL, LH, HL and HH. The LL subband represents the lowest resolution and a half-sized version of the original image. In fact, it is the most significant information for the decoding process (without it, the image cannot be rebuilt), while the remaining subbands contain vertical, horizontal and diagonal details for the decoding process. Such processing produces two groups of relevance, but the LL subband can be transformed again to generate more levels of resolution. Figure 3 presents an original image that is processed by a DWT applied once and twice, resulting in two and three levels of resolution, respectively from left to right.

In Figure 3, a grayscale 256 × 256 pixels image is transformed by DWT, but the $LL_{(2)}$ subband (64 × 64) could be processed again to generate more levels of resolution. Apart from being influenced by the number of times DWT is applied, the resulted subbands are influenced by the coefficients of the lowpass and highpass filters [29–31], resulting in different discrete wavelet transforms.

Figure 3. DWT processing generating two and three levels of resolution.

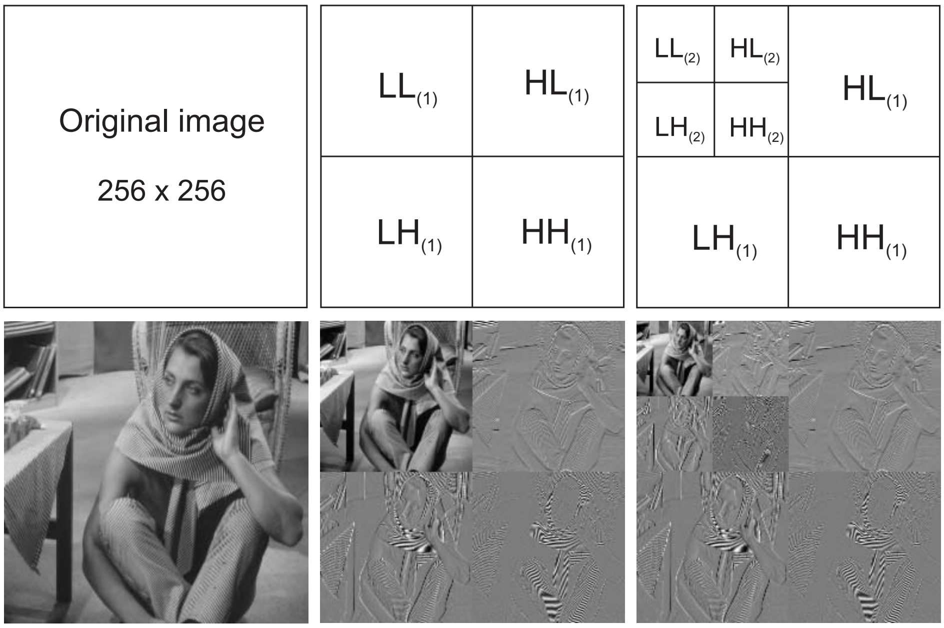

The original image is obtained by performing an inverse DWT over the computed subbands. The lowest resolution representation of the image (the $LL_{(n)}$ subband) is required, while the other subbands will be used to increase the quality of the final image. If the other subbands are lost, the image quality decreases. In fact, the acceptable image quality depends on the application requirements and the expected uses of the retrieved images, but many applications support reduction in the image quality due to changes in the network conditions. We must consider the fact that each bit must be transmitted over the sensor network, which implies energy consumption in the source and over the path(s) toward the sink. Moreover, retransmissions increase such energy consumption. In short, higher quality of received images usually demands more energy resources of the sensor network.

Each packet will be assigned a QoS level according to the packet's payload. As the original images will be processed by 2D DWT, the QoS of each packet depends on the relevance of the produced subbands. The packet's QoS is represented by the Data Relevance (DR), an 8-bit field to be inserted in every transmitted packet, just after the fragmentation header *f*. The value of DR is computed depending on the number of times DWT is applied, which in our proposed solution can be once (1-level) or twice (2-level).

During packet transmission, intermediate nodes will check DR in order to verify the expected reliability level of the packet. In practical terms, the relaying node will check it to decide if a timeout must be set and if an ACK message is expected from the next hop toward the sink, while the receiving node relies on the value of DR to decide if an ACK message must be sent to the previous hop for positive acknowledgment purposes.

Table 1 presents the possible values of DR according to DWT subbands, and the corresponding transmission service. It is interesting to notice that packets carrying data of a single image may experience different reliability guarantees, according to the packet's DR. An important remark is that the image header of the entire image (i_o) must be transmitted with the same priority of $LL_{(n)}$ subbands (highest priority), since it is mandatory for the proper reconstruction of the original image at the receiver side.

Table 1. Values for the Data Relevance.

DR	DWT subbands	Expected level of reliability
0	$LL_{(1)}$, $LL_{(2)}$	Reliable transmission
1–254	$HL_{(2)}$, $LH_{(2)}$, $HH_{(2)}$	Semi-reliable transmission
255	$HL_{(1)}$, $LH_{(1)}$, $HH_{(1)}$	Unreliable transmission

Table 1 gives us a clear notion that most information (75%) will be unreliably transmitted over the network (not retransmitted if corrupted), saving energy avoiding packet retransmissions and transmission of ACK messages. For a 1-level 2D DWT, the proposed solution assures reliable transmission for only 25% of the image information ($LL_{(1)}$), while for a 2-level 2D DWT, only 6.25% of the original visual information ($LL_{(2)}$) will be granted with full reliability guaranties. If packets carrying part of the remaining subbands are lost and not retransmitted, the sink can interpolate the received data to overcome the missing information or consider zeros to complete the subband.

After applying DWT over the original image, the resulting packets should be transmitted in a scrambled order according to their Data Relevance, alternating the packets of highest relevance with low relevant packets. As the occurrence of error bursts is unpredictable (it is estimated only the average errors occurrence), a scrambled transmission may reduce the probability of mass losses of least relevant packets in the worst cases, providing a fairer distribution of retransmission attempts across time.

As a final comment, DWT processing at source nodes demands energy that should be considered when computing the overall energy consumption. Such required energy, C_{pi}, is a direct function of the type (coefficients of the L and H filters) of the employed DWT and it is consumed only in the source node, since we do not consider the energy consumption at the sink. As we are comparing the proposed solution with traditional hop-by-hop retransmission mechanisms, where original images will also need to be processed/coded at source nodes in most cases, we do not consider such energy crucial to the desired analyses. Nevertheless, we compute such energy adapting the corresponding equation in [16], where DWT is performed using a integer 5-tap/3-tap filter. For a m x n image, and considering e_{shift} the energy required for a 1-byte shift operation, e_{add} the energy for an 1-byte add operation, e_{read} the energy to read one byte from memory and e_{write} the energy to write one byte, the computation of C_{pi} is defined in Equation (14), where T is the number of times DWT is applied.

$$C_{Tpi} = \sum_{j=1}^{T}\left(\frac{1}{4^{(j-1)}}.m.n.\left(10.e_{shift} + 12.e_{add} + 2.e_{read} + 2.e_{write}\right)\right) \tag{14}$$

4.2. The Proposed DWT-Based Selective Retransmission Mechanism

We define three levels of reliability according to the value of DR: reliable, unreliable and semi-reliable. Based on the mapping in Table 1, if a 1-level 2D DWT is applied over an original image, packets will be transmitted in a reliable or unreliable way. On the other hand, packets carrying data produced by a 2-level 2D DWT may be transmitted under any of the three reliability levels. The number of times DWT is applied over original images (defining possible values of DR) will indicate the transmission service that must be considered. We will extend the energy consumption model described in Section 3 to incorporate these new definitions.

In reliable transmission, every corrupted packet is retransmitted. For unreliable transmission, no retransmission is performed for the corrupted packet. Finally, in semi-reliable transmission, corrupted packets may be retransmitted depending on where the event occurred. Figure 4 depicts the three different reliability services.

Figure 4. Reliable, semi-reliable and unreliable transmission services.

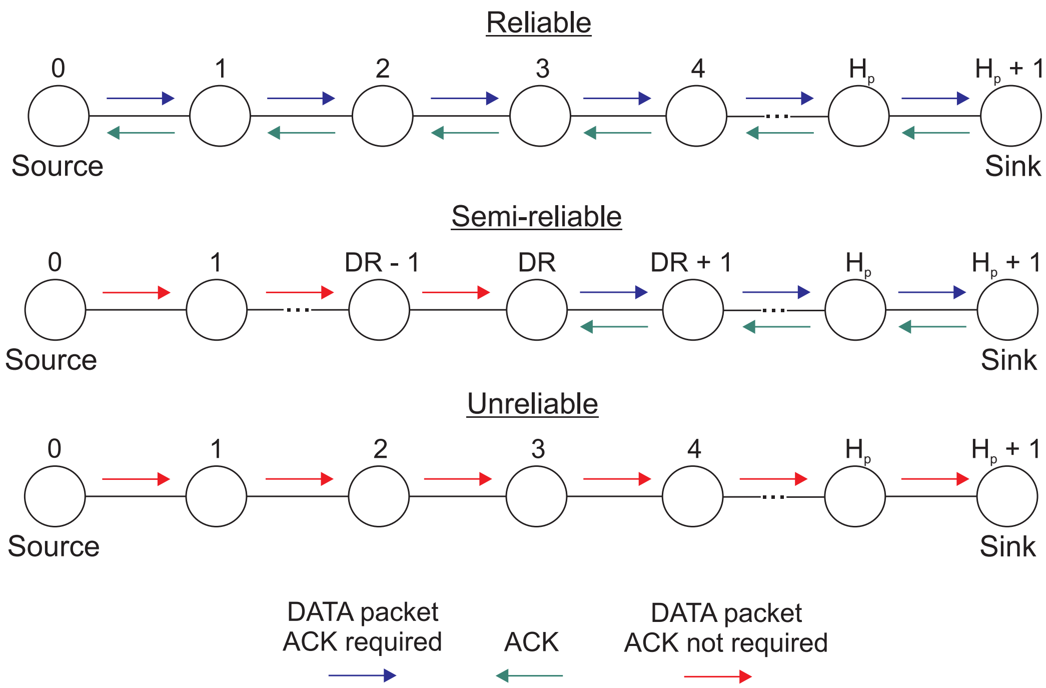

It is considered that an original image i, $i = 1, \ldots, i = I$, sizing B_i bytes may be decomposed by a 2D DWT applied once or twice. Whatever the case, 75% of the resulted data will correspond to the $HL_{(1)}$, $LH_{(1)}$ and $HH_{(1)}$ subbands, and packets containing such data will be unreliably transmitted. We can define U_{pi} as the number of required packets with size s to transmit these three subbands and Lu_{pi} as the size of the payload of the last packet after fragmentation, if any, as expressed in Equation (15). We define l as the maximum payload size in bits of each packet, $l = (s - k - f - 8)$, considering the 8-bit Data Relevance field. The total number of packets carrying data of the $HL_{(1)}$, $LH_{(1)}$ and $HH_{(1)}$ subbands is $U_{pi} + 1$, for $Lu_{pi} > 0$.

$$
\begin{aligned}
U_{pi} &= \left\lfloor \frac{\left\lceil \frac{3*B_i}{4} \right\rceil}{l} \right\rfloor \\
Lu_{pi} &= \left(\left\lceil \frac{3*B_i}{4} \right\rceil - l.\left\lfloor \frac{\left\lceil \frac{3*B_i}{4} \right\rceil}{l} \right\rfloor \right)
\end{aligned}
\qquad (15)
$$

In average, each hop (h + 1) will transmit less packets with DR = 255 to the next hop than hop h transmitted to it, for the same path, since some of them will be lost and not retransmitted. Defining Ptu_{ph} as the packet error rate in hop h when $n = (Lu_{pi} + s - 1)$ in Equation (4), we can estimate the average number of bits to be transmitted from hop h as Tu_{pih}, as presented in Equation (16).

$$Tu_{pih} = \begin{cases} U_{pi}.s.\prod_{j=1}^{h}\left(1 - Pt_{pj}\right), Lu_{pi} = 0 \\ U_{pi}.s.\prod_{j=1}^{h}\left(1 - Pt_{pj}\right) + \left(Lu_{pi} + s - l\right).\prod_{j=1}^{h}\left(1 - Ptu_{pj}\right), Lu_{pi} > 0 \end{cases} \tag{16}$$

A 2D DWT is applied only after the $LL_{(1)}$ subband is produced, representing 25% of the size of the original image. We define M_{pi} as the number of packets for the $LL_{(1)}$ subband and the image header i_o considering that all packets are carrying data to their maximum capacity and Lm_{pi} as the size of the last packet after fragmentation, if any, as presented in Equation (17). The total number of packets carrying data of the $LL_{(1)}$ subband is $M_{pi} + 1$, for $Lm_{pi} > 0$.

$$\begin{aligned} M_{pi} &= \left\lfloor \frac{\left\lceil \frac{B_i}{4} \right\rceil + i_o}{l} \right\rfloor \\ Lm_{pi} &= \left(\left(\left\lceil \frac{B_i}{4} \right\rceil + i_o \right) - l.\left\lfloor \frac{\left(\left\lceil \frac{B_i}{4} \right\rceil + i_o \right)}{l} \right\rfloor \right) \end{aligned} \tag{17}$$

Defining Ptm_{ph} as the packet error rate in hop h when $n = (Lm_{pi} + s - l)$ in Equation (4), we achieve the average number of transmissions of the last packet, Rtm_{ph}, when employing Ptm_{ph} in Equation (8), where $Ptm_{ph} = 0$ and $Rtm_{ph} = 1$ if $Lm_{pi} = 0$. As packets with DR = 0 will be retransmitted if corrupted, Tm_{pih} refers to the total amount of bit transmission (considering possible retransmissions) of subband $LL_{(1)}$ in path p and from hop h to $(h + 1)$. As the probability of ACK transmissions is also affected by the possible smaller size of the last packet, we apply Ptm_{ph} to Equation (10), achieving the average number of ACK messages to acknowledge the transmission of the last packet after fragmentation in hop h of path p, Ram_{ph}, where $Ram_{ph} = 0$ if $Lm_{pi} = 0$. The values of Tm_{pih} and Am_{pih} for the most relevant data (DR = 0) and for a 1-level 2D DWT are defined in Equation (18).

$$\begin{aligned} Tm_{pih} &= \begin{cases} M_{pi}.s.Rt_{ph} + \left(Lm_{pi} + s - l\right).Rtm_{ph}, Lm_{pi} > 0 \\ M_{pi}.s.Rt_{ph}, Lm_{pi} = 0 \end{cases} \\ Am_{pih} &= \begin{cases} a.\left(M_{pi}.Ra_{ph} + Ram_{ph}\right), Lm_{pi} > 0 \\ a.M_{pi}.Ra_{ph}, Lm_{pi} = 0 \end{cases} \end{aligned} \tag{18}$$

When source nodes process gathered images using a 1-level 2D DWT, packets can only be transmitted in a reliable or unreliable way. We can estimate the expected energy consumption in such a case, as presented in Equation (19). For transmission of multiple images, all one has to do is to sum the expected energy consumption in path *p* for each image *i*.

$$\begin{aligned} Et_{pih} &= \left(Tm_{pih} + Tu_{pih}\right).\left(e_e + e_t.d_{ph}^2\right) + Am_{pi(h-1)}.\left(e_e + e_t.d_{p(h-1)}^2\right) \\ Er_{pih} &= \left(Tm_{pi(h-1)} + Am_{pih} + Tu_{pi(h-1)}\right).e_e \end{aligned} \tag{19}$$

The final energy consumption model when images are processed by a 1-level 2D DWT, considering the energy costs of the source node, is presented in Equation (20).

$$E_{pi} = \sum_{h=1}^{H_p}\left(Et_{pih} + Er_{pih}\right) + \left(Tm_{pi0} + Tu_{pi0}\right).\left(e_e + e_t.d_{p0}^2\right) + Am_{pi0}.e_e + C_{1pi} \tag{20}$$

When a 2-level 2D DWT is applied over a raw image, reliable, unreliable and semi-reliable transmission services may be provided according to the resulted subbands. The subbands $HL_{(1)}$, $LH_{(1)}$ and $HH_{(1)}$ present the same visual information of the equivalent subbands after a 1-level 2D DWT, thereby receiving the same treating by intermediate nodes. The subband $LL_{(2)}$ contains the most significant visual information to the reconstruction of the original image, and so the highest relevance (DR = 0) is assigned to it. As the $LL_{(2)}$ subband is only 6.25% of the size of original image, M_{pi} cannot be considered for energy consumption computation in this case. Thus, Z_{pi} is defined as the number of packets for the $LL_{(2)}$ subband, and Lz_{pi} as the size of the payload of the last packet after fragmentation, as presented in Equation (21).

$$\begin{aligned} Z_{pi} &= \left\lfloor \frac{\left\lceil \frac{B_i}{16} \right\rceil + i_o}{l} \right\rfloor \\ Lz_{pi} &= \left(\left(\left\lceil \frac{B_i}{16} \right\rceil + i_o \right) - l.\left\lfloor \frac{\left\lceil \frac{B_i}{16} \right\rceil}{l} \right\rfloor \right) \end{aligned} \tag{21}$$

Defining Ptz_{ph} as the packet error rate in hop *h* when $n = (Lz_{pi} + s - l)$ in Equation (4), we achieve the average number of transmissions of the last packet, Rtz_{ph}, when employing Ptz_{ph} in Equation (8), where $Ptz_{ph} = 0$ and $Rtz_{ph} = 1$ if $Lz_{pi} = 0$. As the probability of ACK transmissions is also affected by the possible smaller size of the last packet, we apply Ptz_{ph} to Equation (10), achieving Raz_{ph}, where $Raz_{ph} = 0$ if $Lz_{pi} = 0$. The values of Tz_{pih} and Az_{pih} are presented in Equation (22).

$$\begin{aligned} Tz_{pih} &= \begin{cases} Z_{pi}.s.Rt_{ph} + \left(Lz_{pi} + s - l\right).Rtz_{ph}, Lz_{pi} > 0 \\ Z_{pi}.s.Rt_{ph}, Lz_{pi} = 0 \end{cases} \\ Az_{pih} &= \begin{cases} a.\left(Z_{pi}.Ra_{ph} + Raz_{ph}\right), Lz_{pi} > 0 \\ a.Z_{pi}.Ra_{ph}, Lz_{pi} = 0 \end{cases} \end{aligned} \tag{22}$$

The subbands $HL_{(2)}$, $LH_{(2)}$ and $HH_{(2)}$ are obtained from a 2D DWT applied over the subband $LL_{(1)}$. We define Q_{pi} as the number of packets with maximum size s for these subbands, and Lq_{pi} as the size of the payload of the last packet after fragmentation, if any, expressed in Equation (23).

$$
\begin{aligned}
Q_{pi} &= \left\lfloor \frac{\left\lceil \frac{3 * B_i}{16} \right\rceil}{l} \right\rfloor \\
Lq_{pi} &= \left(\left\lceil \frac{3 * B_i}{16} \right\rceil - l . \left\lfloor \frac{\left\lceil \frac{3 * B_i}{16} \right\rceil}{l} \right\rfloor \right)
\end{aligned}
\tag{23}
$$

As defined in Table 1, the packets containing part of subbands $HL_{(2)}$, $LH_{(2)}$ and $HH_{(2)}$ will have a DR between 1 and 254. Moreover, they will be subject to a semi-reliable transmission mechanism. Such transmission mechanism assures reliability only when packets are being relaying by some of the intermediate nodes of the path. Considering a path p with H_p intermediate hops, packets will not be retransmitted if they are lost in any intermediate node from the source (h = 0) to the hop DR, 0 < DR <= H_p, and no ACK message has to be transmitted to acknowledge these packets. After hop DR, packets are reliably transmitted to the sink. The idea is to preserve packets that have already been relayed by some hops and consequently consumed energy, considering that such packets have an intermediate impact in the final image quality.

The value for DR may be defined deterministically before deployment or dynamically measuring the number of hops of the path and setting the better value for DR according to the application requirements. If DR > H_p, packets receive the same treatment as when DR = 255. One can notice that, for paths with more than 254 intermediate nodes, the proposed semi-reliable transmission approach cannot be applied. However, typical paths in most real-world wireless sensor networks are expected to be composed of less than 254 hops.

The value of DR will be directly related to the energy consumption and image quality, where higher DR means in average more energy saving at the cost of quality loss of the reconstructed images. In general cases where applications are not concerned with optimization of it, the DR should refer to the middle of the path.

During packet relaying, each intermediate node decrements the value of DR just before transmission to the next hop, when the value of Data Relevance is not 0 or 255. When DR reaches 0, it is assumed that the packet must be reliably transmitted, as is the case for packets carrying $LL_{(1)}$ and $LL_{(2)}$ subbands.

The transmission of Q_{pi} packets requires a partially reliable communication approach, where packets are never retransmitted from h = 0 to h = DR and packets are always retransmitted if corrupted from hop h = DR to $h = (H_p + 1)$, for 0 < DR <= H_p. The average number of bit transmission in hop h for packets with DR from 1 to 254, Tq_{pih}, is presented in Equation (24). Ptq_{ph} represents the average packet error rate in hop h when $n = (Lq_{pi} + s - l)$ in Equation (4) and the average number of transmissions of the last packet after fragmentation is defined as Rtq_{ph}, when employing Ptq_{ph} in Equation (8). Note that $Ptq_{ph} = 1$ and $Rtq_{ph} = 0$ when $Lq_{pi} = 0$.

$$Tq_{pih} = \begin{cases} Q_{pi}.s.\prod_{j=1}^{h}\left(1-Pt_{pj}\right)+\left(Lq_{pi}+s-l\right).\prod_{j=1}^{h}\left(1-Ptq_{pj}\right), h<DR, Lq_{pi}>0 \\ Q_{pi}.s.\prod_{j=1}^{h}\left(1-Pt_{pj}\right), h<DR, Lq_{pi}=0 \\ \left(Q_{pi}.s.\prod_{j=1}^{DR}\left(1-Pt_{pj}\right)\right).Rt_{ph}+\left(\left(Lq_{pi}+s-l\right).\prod_{j=1}^{DR}\left(1-Ptq_{pj}\right)\right).Rtq_{ph}, h\geq DR, Lq_{pi}>0 \\ \left(Q_{pi}.s.\prod_{j=1}^{DR}\left(1-Pt_{pj}\right)\right).Rt_{ph}, h\geq DR, Lq_{pi}=0 \end{cases} \quad (24)$$

The total number of bit transmission for acknowledgment is defined as Aq_{pih}. The hop DR in path p receives ACK messages from hop (DR + 1), but does not transmit ACK to the previous hop (DR – 1). Applying the value of Ptq_{ph} in Equation (10), we achieve the average number of ACK messages to acknowledge the transmission of the last packet after fragmentation received from hop h, h > DR, that is Raq_{ph}. The definitions for Aq_{pih} is presented in Equation (25), where $Raq_{ph} = 0$ if $Lq_{pi} = 0$ and $Aq_{pih} = 0$ for h < DR.

$$Aq_{pih} = \begin{cases} a.\left(Q_{pi}.\prod_{j=1}^{DR}\left(1-Pt_{pj}\right).Ra_{ph}+\prod_{j=1}^{DR}\left(1-Ptq_{pj}\right).Raq_{ph}\right), h\geq DR, Lq_{pi}>0 \\ a.\left(Q_{pi}.\prod_{j=1}^{DR}\left(1-Pt_{pj}\right).Ra_{ph}\right), h\geq DR, Lq_{pi}=0 \end{cases} \quad (25)$$

The computation of the energy consumption due to transmissions and receptions of an image i in hop h of path p, considering original images processed by a 2-level 2D DWT, is defined in Equation (26).

$$\begin{aligned} Et_{pih} &= \left(Tz_{pih}+Tu_{pih}+Tq_{pih}\right)\left(e_e+e_t.d_{ph}^2\right)+\left(Az_{pi(h-1)}+Aq_{pi(h-1)}\right)\left(e_e+e_t.d_{p(h-1)}^2\right) \\ Er_{pih} &= e_e\left(Tz_{pi(h-1)}+Az_{pih}+Tu_{pi(h-1)}+Tq_{pi(h-1)}+Aq_{pih}\right) \end{aligned} \quad (26)$$

The energy consumption of the path is presented in Equation (27). Note that the value for Aq_{pi0} is zero for the source node.

$$E_{pi} = \sum_{h=1}^{H_p}\left(Et_{pih}+Er_{pih}\right)+\left(Tz_{pi0}+Tu_{pi0}+Tq_{pi0}\right).\left(e_e+e_t.d_{p0}^2\right)+Az_{pi0}.e_e+C_{2pi} \quad (27)$$

When a 1-level 2D DWT is applied over the original image, the energy consumption can be estimated using Equation (20). For the 2-level 2D DWT, the equation in Equation (27) must be considered.

4.3. Measuring the Image Quality

When the two proposed DWT-based selective retransmission mechanism is employed in wireless image sensor networks, some packets containing visual information may be lost according to their

Data Relevance and the packet error rate in each link from the source to the sink. The received payloads will be used to reconstruct an approximated version of the original image by an inverse DWT, where we consider that the lost information (if any) will be replaced by zeros for simplicity. As some less relevant packets may be corrupted and discarded during transmission, resulting in energy saving when those packets are not retransmitted and not acknowledged, the final image quality will be typically lower than the original image quality.

The simpler way to assess the quality of an image transmission is to count the number of packets received by the sink. The formulation in Equation (28) presents the average success ratio (S_1) when a 2D DWT is applied only once, where the maximum attainable success ratio is 1.0 when all packets are always retransmitted if lost or no bit-errors occur during transmission. V_0 e V_{255} are the proportion of data received for packets with DR = 0 and DR = 255, respectively.

$$V_0 = 1$$
$$V_{255} = \frac{U_{pi}.l.\prod_{j=1}^{H_p+1}\left(1 - Pt_{pj}\right) + Lu_{pi}.\prod_{j=1}^{H_p+1}\left(1 - Ptu_{pj}\right)}{\left\lceil \frac{B_i * 3}{4} \right\rceil} \tag{28}$$
$$S_1 = \frac{25.V_0 + 75.V_{255}}{100}$$

When we apply a 2-level 2D DWT, we achieve the average success ratio S_2, as presented in Equation (29). Note that we only count packets transmitted before hop DR for V_{DR} (proportion of data received for packets transmitted in a semi-reliable way), since all packets after it are reliably transmitted to the sink.

$$V_{DR} = \frac{Q_{pi}.l.\prod_{j=1}^{DR}\left(1 - Pt_{pj}\right) + Lq_{pi}.\prod_{j=1}^{DR}\left(1 - Ptq_{pj}\right)}{\left\lceil \frac{B_i * 3}{16} \right\rceil} \tag{29}$$
$$S_2 = \frac{6.25.V_0 + 18.5.V_{DR} + 75.V_{255}}{100}$$

S_1 and S_2 show the average percentage of received data when compared with the total visual information of the original image, but do not give us a good indication of the quality of the reconstructed image, since the packets' payloads have different relevancies for the reconstruction of the original image. A common approach to measure such quality is the Peak Signal-to-Noise Ratio (PSNR), as defined in Equation (30). The value for x is the number of bits to represent a pixel: for example, every pixel in a grayscale image may be represented by 8 bits, but more bits are required for RGB color images.

$$PSNR_{pi} = 10\log_{10}\frac{\left(2^x - 1\right)^2}{MSE_{pi}} \tag{30}$$

The variable MSE_{pi} is the mean squared error, considering an original m x n image i and a final m x n image v, where the last one is a noisy approximation of the original image. Considering that $i(a,b)$ and $v(a,b)$ return the value of the corresponding pixel in position (a,b) of the image, $0 < a < m$ and $0 < b < n$, we have the definition of MSE_{pi} in Equation (31).

$$MSE_{pi} = \frac{1}{m.n} \sum_{a=0}^{m-1} \sum_{b=0}^{n-1} \left[i(a,b) - v(a,b) \right]^2 \tag{31}$$

The closer to the original is the reconstructed image, higher is the $PSNR_{pi}$. In fact, PSNR is a good measure for comparing reconstruction results for the same image, but it is meaningless for comparisons between images, since one image with lower PSNR may look much better than another image with higher PSNR. In the improbable case that no packet is discarded in any link during the transmission of the image i from the source to the sink, due to the absence of error bursts, the value for MSE_{pi} is 0, and the $PSNR_{pi}$ is undefined.

4.4. Conceptual Location of the Proposed Solution

Packet retransmission can be usually performed in two logical layers: link and transport. Some MAC protocols provide a reliable service where lost packets are retransmitted in a hop-by-hop manner, as performed by the IEEE 802.15.4. On the other hand, most transport protocols provide an end-to-end reliable communication service where retransmission requests are sent by the sink. However, the energy constraints of sensor networks fostered the development of hop-by-hop transport protocols, disrupting the traditional protocol modularization. An interesting discussion about the appropriate layer where packet retransmission should be performed is presented in [13].

In such contexts, we believe that the proposed selective retransmission mechanisms can be employed in MAC or transport layers alike, since the hop-by-hop paradigm is respected for higher energy efficiency. For solutions based on link-layer, the IEEE 802.15.4 or T-MAC protocols could be adapted to support selective retransmission based on the data relevance of the packets. For transport protocols, errors not treated by lower protocol layers but that must to be corrected due to the value of DR would result in retransmission requests at the current hop. Alternatively, selective retransmission could be employed in conjunction with both layers, but the final solution should be designed to allow the cooperative operation of the employed protocols. Whatever the case, the same energy and quality analyses discussed in this paper are valid.

5. Numerical Results

Previous section defined comprehensive energy consumption models for the proposed energy-efficient selective retransmission mechanism, where DWT image coding is exploited to produce visual data with different relevancies for the application. Based on the presented equations, we conducted a series of mathematical verifications in Matlab to compare the mean performance of the proposed solution with a fully-reliable transmission mechanism. As we argue that the proposed solution can replace existing approaches for reliable communications in wireless image sensor networks, we are indeed concerned with the gains over traditional solutions, instead of absolute performance values. Moreover, the quality of the reconstructed image is simulated when some packets are lost, computing the average success ratio and the equivalent PSNR.

For the experiments, the transmission of a single uncompressed 128 × 128 8-bit grayscale image was considered, as presented in Figure 5. The image size in question was 16,384 bytes plus an image header of 40 bytes, since the transmission of bitmap images was considered, and 40 bytes is the most common size of bitmap image headers. Thus, $B_i + i_o = 16{,}424$ bytes. The maximum packet size is 127 bytes ($s = 127 \times 8$ bits), the total protocol headers is defined as 30 bytes ($k = 30 \times 8$ bits), the fragmentation header was defined having 8 bytes ($f = 8 \times 8$ bits) and DR sizes 1 byte, as expected. So, in the mathematical verifications, $l = 88$ bytes. We also define $a = 40$ bytes.

Figure 5. Original image for the experiments.

5.1. Energy Consumption

The energy consumption for processing/transmission of every single bit depends on the hardware characteristics of the employed sensors. However, such characteristics do not affect the experiments, since they will be considered for all tests. The parameters for energy consumption computation are based on [15,21], as presented in Table 2.

Table 2. Parameters for the experiments.

Variable	Value
e_e	50×10^{-9} J/bit
e_t	100×10^{-12} J/bit/m^2
e_{shift}	3.3 nJ
e_{add}	3.3 nJ
e_{read}	0.26 µJ
e_{write}	4.3 µJ

The DWT processing in each source node for the image in Figure 5 consumes 150.6 mJ for a 1-level 2D DWT and 188.3 mJ for a 2-level 2D DWT, when the parameters in Table 2 are considered. Such energy is always accounted when assessing the energy consumption of the proposed approach.

Initially, we analyzed the energy consumption as a function of the number of hops that compose the path from the source to the sink. For simplicity, we considered that all nodes have the same transmission range (50 meters), and the previous ($h - 1$) and next ($h + 1$) hops are both in the transmission range of hop h.

Figure 6(a) shows the overall energy consumption (mJ) when the mean PER is 5% (b = 0.9994 and g = 0.99998) for all links between neighbor intermediate nodes, while Figure 6(b) considers the mean PER of 15% (b = 0.99987 and g = 0.99998). Three different transmission approaches were considered: fully-reliable, selective retransmission for 1-level 2D DWT and selective retransmission for 2-level 2D DWT, respectively based on equations in Equations (6), (20) and (27). For the subbands $HL_{(2)}$, $LH_{(2)}$ and $HH_{(2)}$ produced by a 2-level 2D DWT in both tests, DR = (H_p/2). It is also assumed that all packets are transmitted with DR=0 for the traditional fully-reliable transmission approach.

Figure 6. Energy consumption over the path.

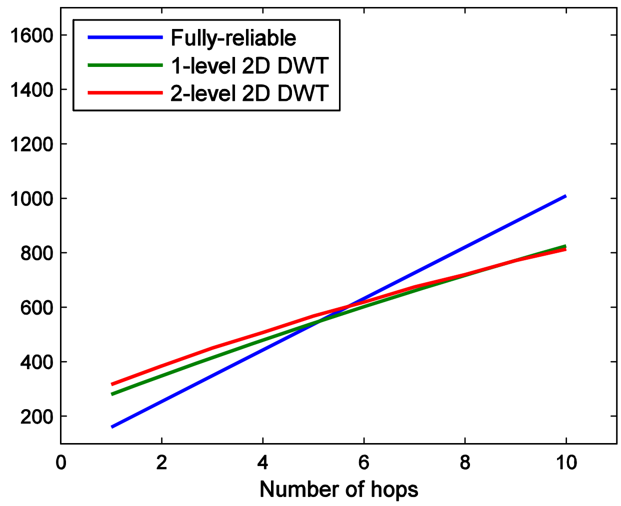

(**a**) Mean PER is 5%.

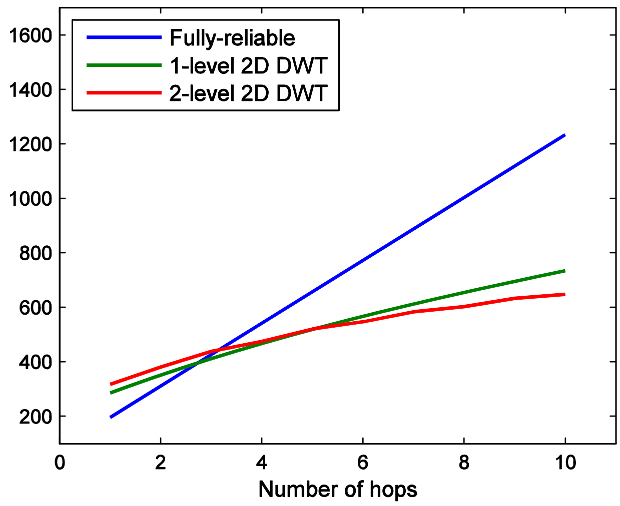

(**b**) Mean PER is 15%.

The initial obvious conclusion is that the energy consumption increases when packets have to cross more intermediate nodes. Moreover, it is interesting to note that higher PER results in energy saving for the proposed approach when compared with the lower PER case, as most data (75%) are unreliably transmitted (DR = 255) over the path, in a different way of the fully-reliable approach.

As we did not consider the energy costs of any coding technique for the fully-reliable transmission mechanism, the proposed solution is less energy-efficient for communications over very short paths, since DWT energy costs have to be accounted. However, such behavior changes when packets have to cross more hops, and it is more evident for higher mean PER. Additionally, even following the fully-reliable paradigm some image coding may be required, also demanding energy of source nodes. There is also an interesting difference between transmissions for packets generated after 1-level and 2-level 2D DWT. The transmission of packets using the semi-reliable transmission service is only advantageous for larger paths and for higher PER, since 2-level 2D DWT consumes more energy than 1-level 2D DWT.

When the fully-reliable transmission mechanism is employed, we expect that, on average, every intermediate node consumes an equivalent amount of energy. However, the energy consumption in each intermediate node is likely to be different for the proposed selective retransmission mechanism, since packets that are lost and not retransmitted in previous hops do not consume energy in subsequent hops in the path to the sink. Considering the same mean PER of the last experiments, Figure 7 presents the energy consumption (mJ) in each hop for a path with 10 intermediate nodes, testing three different values of DR for semi-reliable transmission. For the fully-reliable approach, the average consumed energy in each hop is 94.60 mJ for a mean PER of 5% and 115.12 mJ for a mean PER of 15%.

Figure 7. Energy consumption in each intermediate node.

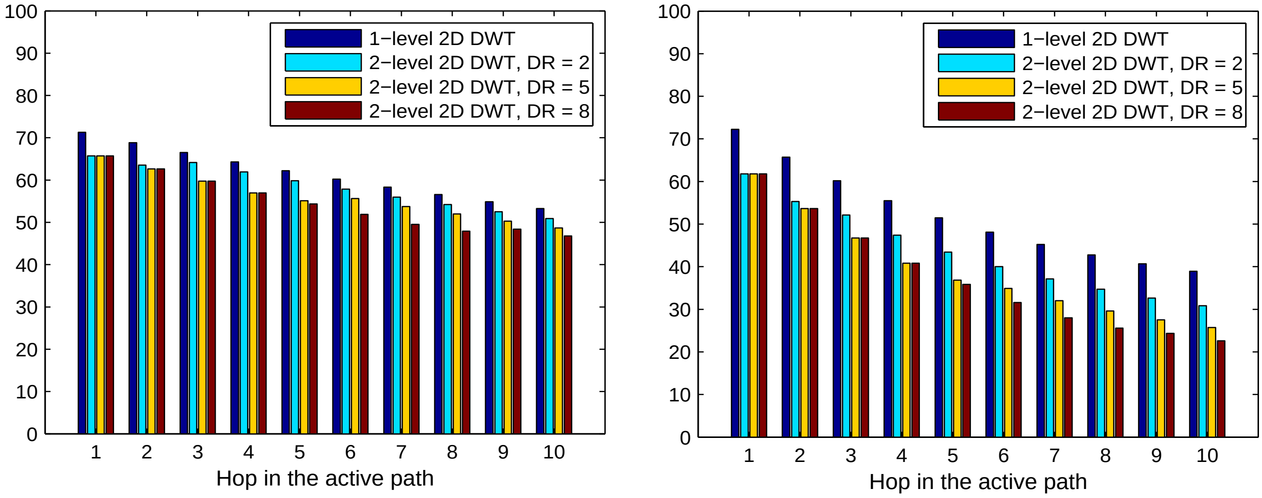

(**a**) Mean PER is 5%. (**b**) Mean PER is 15%.

In both graphics in Figure 7, the 1-level 2D DWT approach always consumes more energy since only packets with DR = 255 are not retransmitted. For the retransmission mechanism based on 2-level 2D DWT, packets with DR = 2, DR = 5 and DR = 8 are also not retransmitted if lost in hops before the hop DR. Another interesting observation is that nodes closer to the sink always consume less energy, and such a difference is more evident for a higher mean PER. As intermediate nodes closer to the sink tend to consume more energy due to the fact that they receive more combined upstream traffic, the proposed retransmission approach may considerably preserve such nodes, potentially prolonging the network lifetime. Finally, note the energy consumption for different values of DR. For low mean packet error rates, the additional energy consumption for ACK transmissions and packet retransmissions is significant, as can be seen in hops 3, 6 and 9 in Figure 7(a) when DR is equal to 2, 5 and 8, respectively. For higher mean PER, the energy saving avoiding reception and relaying of packets that are lost and not retransmitted in previous hops is more significant than additional transmission of ACK messages and packet retransmissions, as can be seen in Figure 7(b).

Besides the relation between energy consumption and number of hops, we can also relate energy with the mean packet error rate, as presented in Figure 8. In that graphic, the active used path is composed of 10 intermediate hops and DR = 5 for the 2-level 2D DWT. Moreover, the considered PER is for packets sizing *s* bits, where *g* and *b* assume different values, resulting in mean PER from 2% to 20%, although we also computed the PER for smaller packets when necessary.

As one can see in Figure 8, the fully-reliable transmission mechanism is severely affected by higher packet error rate, directly impacting the expected network lifetime. For the proposed selective retransmission mechanism, the impact in the expected average energy consumption is considerably lower than traditional fully-reliable transmission approaches, where all packets have the same treatment by intermediate nodes. Once again, it is worth noting that, while energy consumption rises when packets have to cross links with higher PER for the fully-reliable transmission approach, the average energy consumption decreases for the proposed selective retransmission mechanism, considering the same network conditions. Also as expected, the image transmission after a 2-level 2D DWT consumes less energy than the retransmission mechanism based on 1-level 2D DWT, for DR = 5 and $H_p = 10$, and this difference increases for higher mean PER.

Figure 8. Energy consumption for a path composed of 10 intermediate nodes.

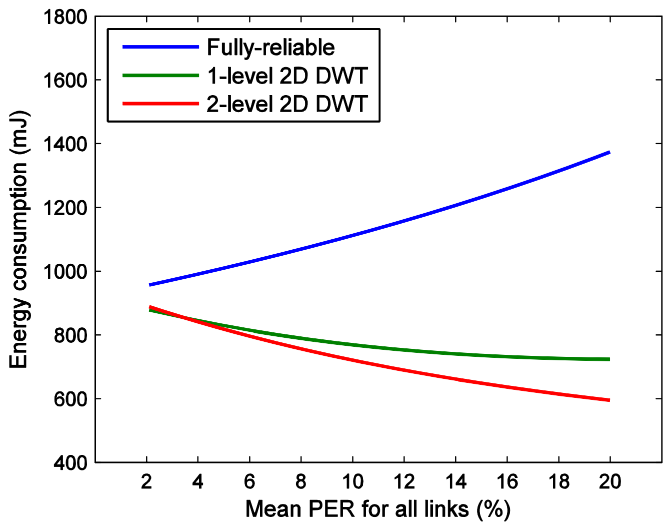

We can also analyze the effect of the value of DR for a 2-level 2D DWT. In Figure 9, we show the total energy consumption for a path composed of 20 hops when an image is transmitted employing the proposed retransmission mechanism based on 2-level 2D DWT, considering different values of DR for the $HL_{(2)}$, $LH_{(2)}$ and $HH_{(2)}$ subbands. Lower DR implies in more energy consumption, since packets will be transmitted with reliability guarantees over a bigger part of the path.

Figure 9. Energy consumption for different values of Data Relevance (DR).

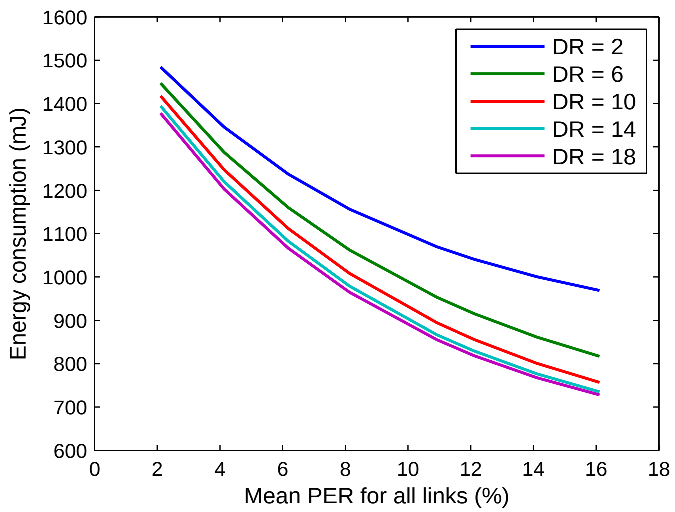

At last, we estimated the effect of a higher packet error rate in some links of the path. Considering a path composed of 20 intermediate nodes, we established a very low 2% PER for all links except in the middle of the path, where higher mean PER were simulated. As the links between hops 9 and 11 experienced a higher packet error rate, it was also verified the effect of the proposed retransmission mechanism for 2-level 2D DWT, considering DR before (DR = 5) an after (DR = 15) the region with increased PER. The results of this experiment are presented in Figure 10.

Figure 10. Energy consumption for a path with different mean packet error rates.

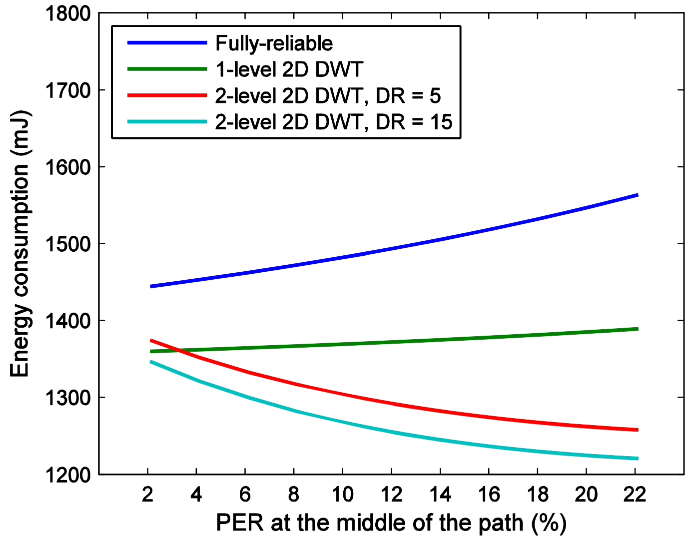

As previously attested, we note in Figure 10 that the proposed selective retransmission mechanism performs better than traditional fully-reliable transmission approaches, saving energy of intermediate nodes. Moreover, such saved energy is higher when a 2-level 2D DWT is applied over the original image, especially when DR = 15 for $HL_{(2)}$, $LH_{(2)}$ and $HH_{(2)}$ subbands. An interesting consideration is that the selective retransmission mechanism based on 1-level 2D DWT consumes more energy for higher mean PER at the middle of the path, even though fewer packets with DR = 255 will need to be transmitted on average over half the path. This happens because packets with DR = 0 will require on average more retransmissions and transmission of ACK messages, impacting the resulting energy consumption.

5.2. Image Quality

The simplest way to measure the quality of the reconstructed image is the success ratio. We initially used the same parameters of the experiments of Figure 6 to compute the success ratios, as depicted in Figure 11. As expected, more packets are lost on average when the current used path is composed of more hops.

Figure 11. Success ratios for different mean packet error rates.

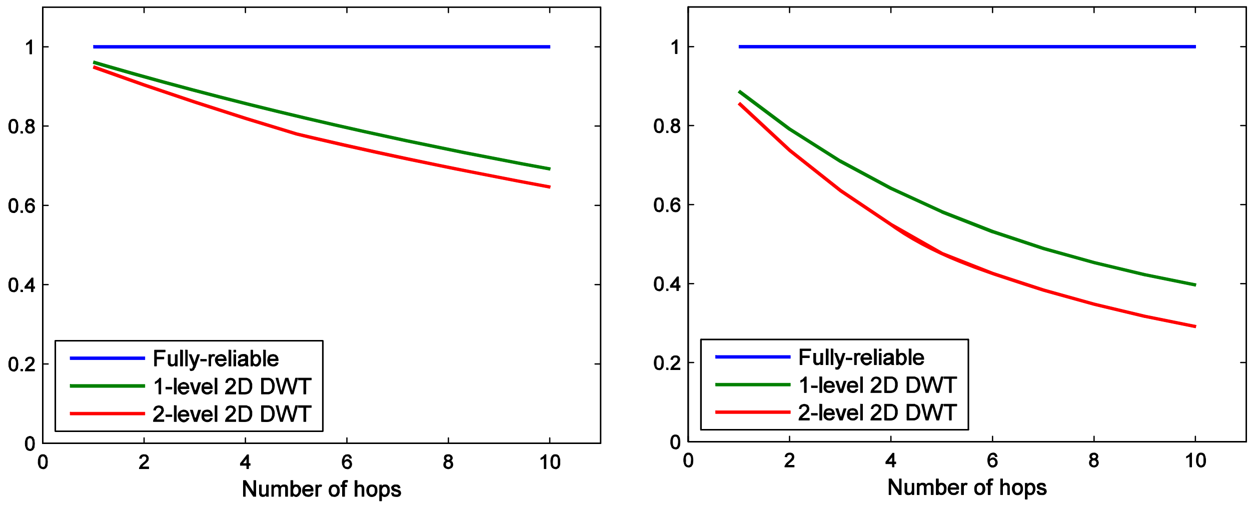

(**a**) Mean PER is 5%. (**b**) Mean PER is 15%.

We can also relate the success ratio with the mean packet error rate, as presented in Figure 12, where a path composed of 10 intermediate nodes is considered. Note that success ratio is severely affected by higher PER. An interesting consideration is that the 2-level 2D DWT based retransmission approach consumes less energy, but results in higher mean packet loss, especially for values of DR closer to the sink.

Figure 12. Success ratio *versus* PER.

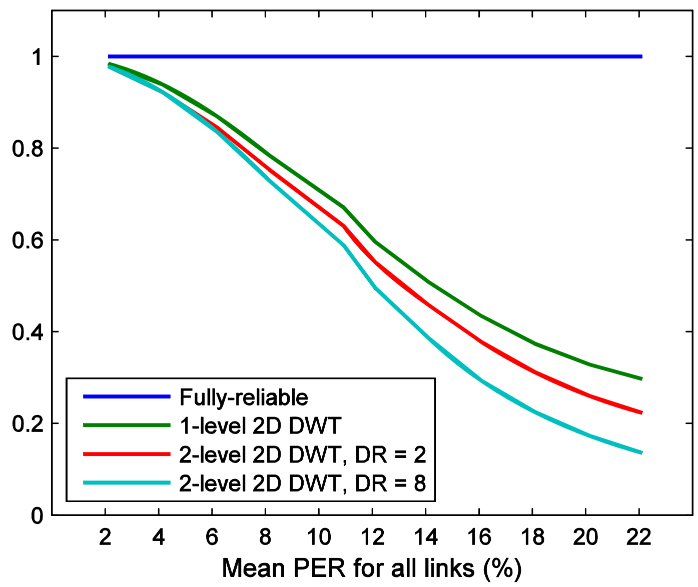

The success ratio presents the expected mean packet loss, but does not provide a direct value for the image quality, since packets have different relevancies for the reconstruction of the image at the receiver side. In order to have a better feeling of the resulted image quality, we estimated some packet loss and computed the PSNR of the reconstructed image.

Figure 13 presents the image quality after transmission considering the 1-level 2D DWT based approach, where packets with DR = 255 may be lost. In that figure, we simulated different percentage of packet loss, including the worst case when all packets with DR = 255 are lost. A total of 140 packets with DR = 255 are transmitted for the original image of Figure 5.

Figure 13. Visual quality and Peak Signal-to-Noise Ratio (PSNR) after loss of packets with DR = 255 and 1-level 2D DWT.

Loss of 5% (7 packets)	Loss of 20% (28 packets)	Loss of 40% (56 packets)
Success ratio 0.9625	Success ratio 0.85	Success ratio 0.7
PSNR 31.09 dB	PSNR 30.96 dB	PSNR 30.09 dB

Loss of 60% (84 packets)	Loss of 80% (112 packets)	Loss of 100% (140 packets)
Success ratio 0.55	Success ratio 0.4	Success ratio 0.25
PSNR 26.32 dB	PSNR 24.98 dB	PSNR 24.23 dB

Analyzing the reconstructed images it can be seen that, even in the worst case, the visual quality seems to be very acceptable for many types of wireless image sensor networks applications. And if so, we noted that the energy saving is highly significant when the retransmission approach based on 1-level 2D DWT is applied, strongly benefiting such applications.

We also analyzed the impact of loss of packets with DR = 255 when some packets with DR > 0 and DR < 255 are also lost. Figure 14 presents the resulted images considering 20% of loss of packets carrying the $HL_{(2)}$, $LH_{(2)}$ and $HH_{(2)}$ subbands (totalizing 7 packets), considering that 35 packets of such packets are transmitted.

Figure 14. Visual quality and PSNR after loss of packets with DR = 255 and 2-level 2D DWT. It is assumed that 20% of packets with 0 < DR < 255 are lost.

Loss of 5% (7 packets)
Success ratio 0.9625
PSNR 28.20 dB

Loss of 20% (28 packets)
Success ratio 0.85
PSNR 26.18 dB

Loss of 40% (56 packets)
Success ratio 0.7
PSNR 26.12 dB

Loss of 60% (84 packets)
Success ratio 0.55
PSNR 25.58 dB

Loss of 80% (112 packets)
Success ratio 0.4
PSNR 24.55 dB

Loss of 100% (140 packets)
Success ratio 0.25
PSNR 23.82 dB

After a 2-level 2D DWT, the $HL_{(2)}$, $LH_{(2)}$ and $HH_{(2)}$ subbands are more significant for the reconstruction of the image than the $HL_{(1)}$, $LH_{(1)}$ and $HH_{(1)}$ subbands. We can note in Figure 14 that the loss of only 20% of packets with DR > 0 and DR < 255 negatively impact the image quality, as can be seen by the computed PSNR. Such a negative impact is more severe for ~50% of loss of such packets (totaling 17 packets), as presented in the images in Figure 15.

Figure 15. Visual quality and PSNR after loss of packets with DR = 255 and 2-level 2D DWT. Almost 50% of packets with 0 < DR < 255 are lost.

Loss of 5% (7 packets)
Success ratio 0.9625
PSNR 21.6 dB

Loss of 20% (28 packets)
Success ratio 0.85
PSNR 21.34 dB

Loss of 40% (56 packets)
Success ratio 0.7
PSNR 22.86 dB

Figure 15. *Cont.*

Loss of 60% (84 packets)	Loss of 80% (112 packets)	Loss of 100% (140 packets)
Success ratio 0.55	Success ratio 0.4	Success ratio 0.25
PSNR 22.69 dB	PSNR 22.08 dB	PSNR 21.66 dB

In this last case, we can note the lower quality of the reconstructed images, which may harm the visual monitoring capability of the application. One should notice, however, that images that look better may have a lower PSNR, since it is a way to measure the quality of the reconstructed images when compared with the original image, and thus it is useless to make comparisons between reconstructed images.

The impact when packets with $0 < DR < 255$ are lost are very severe for the quality of the reconstructed image, but the energy saving when compared with the 1-level 2D DWT retransmission approach is not as significant as the loss of the image quality. After the performed analyses and mathematical verifications, we concluded that if the application cannot afford higher loss of quality of the reconstructed images, the semi-reliable transmission service should not be considered for the application, leading source nodes to apply only 1-level 2D DWT over original images.

As a final comment, one may argue that if the application can afford some packet loss, it is better to discard packet at the source, avoiding transmission of less relevant information. However, such an approach would result in low quality images even when the packet error rates of the links are low. The proposed selective retransmission mechanism is more adequate to real-world applications where errors happen as burst, saving energy and keeping an acceptable average image quality over time.

6. Conclusions

In this paper we have proposed a DWT-based energy-efficient selective retransmission mechanism for wireless image sensor networks, where packets are transmitted with different reliability guarantees according to the relevancies of the packets' payloads for the reconstruction of the original image at the receiver side. We designed comprehensive energy consumption models and performed extensive mathematical verifications, estimating the average energy consumption and the resulted image quality when some less relevant packets are lost.

When applications can afford some loss in the image quality, it was showed that the proposed solution performs better than traditional fully-reliable transmission mechanisms, achieving considerable energy saving in intermediate nodes. Moreover, we noted that the visual quality of the received images may be highly acceptable in different error conditions, especially for the 1-level 2D DWT based selective retransmission approach. In fact, the conclusions are based on the average cases, which although not sufficient to attest the effectiveness of the proposed solution, present an average behavior that can be expected in most cases along the time. The performed mathematical verifications have brought numeric values that indicated better options in average, turning the proposed solution promising for wireless image sensor networks. Nevertheless, future works will be concerned with experimental verifications in a discrete event simulator featuring IEEE 802.15.4 MAC technology, in order to allow analyzes of punctual values of error rate, retransmission attempts and energy consumption in more realist communication scenarios. In fact, transmissions using duty-cycle contention-based protocols are controlled by messages as RTS and CTS and generally synchronization messages are transmitted among the nodes to optimize the sleeping time, adding new issues to the energy consumption estimation.

Image transmissions over wireless sensor networks may be challenging when resource-constrained sensor nodes are deployed. The huge amount of information that has to cross the network considerably increases the energy consumption over the network, when compared with traditional scalar wireless sensor networks. A reasonable solution to address such particular issue is to compress data before transmission [29,31,32]. Future works will investigate how compression strategies can be combined with the proposed solution: if DWT is applied over original images, the resulted subbands could be compressed to reduce the number of packets to be transmitted, but still allowing differentiated transmission services according to the value of DR. We expect that the adoption of compression algorithms can reduce the overall energy consumption of the network, but the proportional gains of the proposed solution over fully-reliable transmission approaches should remain if packets can still be classified according to the payload relevance for the reconstruction of the original images.

Moreover, we envisage that the proposed selective retransmission mechanism can be employed as part of a global solution, addressing issues as network congestion and node failure. Dynamic adaptation of parameters of the retransmission procedures can be performed according to the current network conditions. At last, although it is expected that many wireless image sensor network applications are delay-tolerant, we intend to investigate the potential benefits of the proposed selective retransmission mechanism for the end-to-end delay of the communication. As the use of ACK messages for acknowledgment and retransmission procedures demand additional time, the proposed solution may reduce the overall delay of the communication, potentially benefiting real-time WISN applications.

References

1. Yick, J.; Mukherjee, B.; Ghosal, D. Wireless sensor network survey. *Comput. Netw*. **2008**, *52*, 2292–2330.
2. Akyildiz, I.; Su, W.; Sankarasubramaniam, Y.; Cayirci, E. Wireless sensor networks: A survey. *Comput. Netw.* **2002**, *38*, 393–422.
3. Baronti, P.; Pillai, P.; Chook, V.; Chessa, S.; Gotta, A.; Hu, Y. Wireless sensor networks: A survey on the state of the art and the 802.15.4 and ZigBee standards. *Comput. Commun*. **2006**, *30*, 1655–1695.
4. Almalkawi, I.; Zapata, M.; Al-Karaki, J.; Morillo-Pozo, J. Wireless multimedia sensor networks: Current trends and future directions. *Sensors* **2010**, *10*, 6662–6717.

5. Misra, S.; Reisslein, M.; Xue, G. A survey of multimedia streaming in wireless sensor networks. *IEEE Commun. Surv. Tutor.* **2009**, *10*, 18–39.
6. Soro, S.; Heinzelman, W. On the Coverage Problem in Video-Based Wireless Sensor Networks. In *Proceedings of the International Conference on Broadband Networks*, Boston, MA, USA, 3–7 October 2005; pp. 932–939.
7. Soro, S.; Heinzelman, W. A survey of visual sensor networks. *Adv. Multimed*. **2009**, *2009*, 1–21.
8. Charfi, Y.; Canada, B.; Wakamiya, N.; Murata, M. Challenging issues in visual sensor networks. *IEEE Wirel. Commun.* **2009**, *16*, 44–49.
9. Costa, D.; Guedes, L. The coverage problem in video-based wireless sensor networks: A survey. *Sensors* **2010**, *10*, 8215–8247.
10. Costa, D.; Guedes, L. A survey on multimedia-based cross-layer optimization in visual sensor networks. *Sensors* **2011**, *11*, 5439–5468.
11. Akyildiz, I.; Melodia, T.; Chowdhury, K. A survey on wireless multimedia sensor networks. *Comput. Netw.* **2007**, *51*, 921–960.
12. Boukerche, A.; Du, Y.; Feng, J.; Pazzi, R. A Reliable Synchronous Transport Protocol for Wireless Image Sensor Networks. In *Proceedings of IEEE Symposium on Computers and Communications*, Marrakesh, Morocco, 6–9 July 2008; pp. 1083–1089.
13. Stann, F.; Heidemann, J. RMST: Reliable Data Transport in Sensor Networks. In *Proceedings of International Workshop on Sensor Network Protocols and Applications*, Anchorage, AK, USA, 11 May 2003; pp. 102–112.
14. Liu, Y.; Huang, H.; Xu, K. Multi-path-based Distributed TCP Caching for Wireless Sensor Networks. In *Proceedings of International Conference on Software Engineering, Artificial Intelligence, Networking and Parallel/Distributed Computing*, Phuket, Thailand, 6–8 August 2007; pp. 331–335.
15. Wu, H.; Abouzeid, A. Error resilient image transport in wireless sensor networks. *Comput. Netw.* **2006**, *50*, 2873–2887.
16. Lecuire, V.; Duran-Faundez, C.; Krommenacker, N. Energy-efficient transmission of wavelet-based images in wireless sensor networks. *EURASIP J. Image Video Process.* **2007**, *2007*, 1–11.
17. Lee, J.-H.; Jun, I.-B. Adaptive-compression based congestion control technique for wireless sensor networks. *Sensors* **2010**, *10*, 2919–2945.
18. Dam, T.; Langendoe, K. An Adaptive Energy-Efficient MAC Protocol for Wireless Sensor Networks. In *Proceedings of ACM SenSys*, Los Angeles, CA, USA, 5–7 November 2003; pp. 1–10.
19. Korhonen, J.; Wang, Y. Effect of Packet Size on Loss Rate and Delay in Wireless Links. In *Proceedings of IEEE Wireless Communications and Networking Conference*, New Orleans, FL, USA, 13–17 March 2005; pp. 1608–1613.
20. Pekhteryev, G.; Sahinoglu, Z.; Orlik, P.; Bhatti, G. Image Transmission over IEEE 802.15.4 and ZigBee Networks. In *Proceedings of IEEE International Symposium on Circuits and Systems*, Kobe, Japan, 23–26 May 2005; pp. 539–3542.
21. Lecuire, V.; Duran-Faundez, C.; Krommenacker, N. Energy-efficient image transmission in sensor networks. *Int. J. Sens. Netw*. **2008**, *4*, 37–47.
22. Qaisar, S.; Radha, H. Multipath Multi-stream Distributed Reliable Video Delivery in Wireless Sensor Networks. In *Proceedings of Conference of Information Sciences and Systems*, Baltimore, MA, USA, 18–20 March 2009; pp. 207–212.

23. Liang, Y.; Peng, W. Minimizing energy consumptions in Wireless sensor networks via two-modal transmission. *ACM SIGCOMM Comput. Commun. Rev*. **2010**, *40*, 12–18.
24. Demirkol, I.; Ersoy, C.; Alagöz, F. MAC protocols for wireless sensor networks: A survey. *IEEE Commun. Mag*. **2006**, *44*, 115–121.
25. Garcia-Sanchez, A.-J.; Garcia-Sanchez, F.; Garcia-Haro, J.; Losilla, F. A cross-layer solution for enabling real-time video transmission over IEEE 802.15.4 networks. *Multim. Tools App*. **2011**, *51*, 1069–1104.
26. Han, B.; Lee, S. Efficient Packet Error Rate Estimation in Wireless Networks. In *Proceedings of Conference on Testbeds and Research Infrastructure for the Development of Networks and Communities*, Orlando, FL, USA, 21–23 May 2007; pp. 1–9.
27. Dunkels, A.; Alonso, J.; Voigt, T.; Ritter, H. Distributed TCP Caching for Wireless Sensor Networks. In *Proceedings of Annual Mediterranean Ad Hoc Networking Workshop*, Bodrum, Turkey, 27–30 June 2004; pp. 1–11.
28. Shon, T.; Choi, H. Towards the implementation of reliable data transmission for 802.15.4-based wireless sensor networks. *Lecture Notes Comput. Sci*. **2008**, *5061*, 363–372.
29. Chew, L.; Ang, L.-M.; Seng, K. Survey of Image Compression Algorithms in Wireless Sensor Networks. In *Proceedings of International Symposium on Information Technology*, Kuala Lumpur, Malaysia, 26–28 August 2008; pp. 1–9.
30. Antonini, M.; Barlaud, M.; Mathieu, P.; Daubechies, I. Image coding using wavelet transform. *IEEE Trans. Image Process*. **1992**, *1*, 205–220.
31. Lee, D.; Dey, S. Adaptive and Energy Efficient Wavelet Image Compression for Mobile Multimedia Data Services. In *Proceedings of IEEE International Conference on Communications*, New York, USA, 28 April-2 May 2002; pp. 2484–2490.
32. Duran-Faundez, C.; Lecuire, V.; Lepage, F. Tiny block-size coding for energy-efficient image compression and communication in wireless camera sensor networks. *Signal Process. Image Commun*. **2011**, *26*, 466–481.